INVESTIGATIONS OF OCEAN REFLECTANCE WITH AVIRIS DATA

STUART H. PILORZ and CURTISS 0. DAVIS
Jet Propulsion Laboratory, California Institute of Technology
M/S 300-323, 4800 Oak Grove Dr., Pasadena, California, 91109, USA

ABSTRACT

Multispectral imagery with the resolution of the Airborne Visible/Infrared Imaging Spectrometer (AVIRIS) offers the possibility for retrieving concentrations of in-water constituents in turbid and coastal waters inaccessible to instruments of low spectral and spatial resolution. The oceanography group at the Jet Propulsion Laboratory (JPL) is involved in an ongoing experiment at Monterey Bay, California, coupling AVIRIS overflights with in-situ data for development of spectral unmixing algorithms suitable for AVIRIS and the High Resolution Imaging Spectrometer (HIRIS). Given the low signal emitted by water, a large portion of the developmental work has centered on defining signal-to-noise characteristics necessary for separation of spectral endmembers. Although AVIRIS was not originally designed for ocean viewing, several improvements have been made in the data processing and acquisition, as well as to the instrument itself, which put AVIRIS on the borderline of detection requirements for estimation of chlorophyll concentrations. Further modifications have been proposed which would increase the S/N by a factor of 2 to 4 in the blue regions of the spectrum enabling use of the instrument for spectral unmixing of pigments, chlorophyll, and suspended sediments. This paper documents the present capabilities of AVIRIS for ocean studies and quantifies the need for improved S/N in the visible part of the spectrum.

INTRODUCTION

Quantitative evaluation of the concentrations of constituents within a body of water has many uses, ranging from analysis of pollutants and eutrophication in lakes and estuaries to estimation of carbon production in the ocean [JGOFS, 1988]. The dominant factor affecting the remote sensing reflectance of waters of slight to moderate turbidity is the bulk absorption of the water column. For the open ocean, surface chlorophyll concentrations have been regressed against ratios of reflected radiance taken for pairs of frequencies, but the larger number of absorbers in coastal waters (Figure 1) make this method unreliable in that environment. Specifically, with only a few bands and limited S/N, it becomes impossible even to deconvolve the effects of suspended sediment from those of chlorophyll on the reflected radiance. Also, differences in the carbon fixing capabilities of different phytoplankton groups relative to their chlorophyll content make it desirable to discriminate between them, or at least to discriminate between the concentration of chlorophyll itself and that of related pigments.

Analysis of in-water constituents that utilize the capabilities of an instrument such as AVIRIS hinges upon the development of a wavelength-dependent model expressing the reflected radiance as a function of the optical properties of the water column. This entails modelling the effects of the optical properties of individual particles or classes of particles upon the bulk absorption and scattering properties of the water column. Significant literature exists involving application of radiative transfer methods to hydrologic optics [Preisendorfer, 1976; Kirk, 1983], as well as dealing with Monte Carlo simulation of water optical properties [Gordon et al, 1975; Kirk, 1981]. A model consistent with both of the above expresses the water reflectance as being proportional to the bulk backscattering and

inversely proportional to the absorption properties of the water column [Morel and Prieur, 1977] :

$$R = k \cdot b_b / (b_b + a) \quad (1)$$

Here R represents the reflectance at a wavelength, b_b the bulk backscattering, and a the bulk absorption of the water column at that wavelength. The constant k has been empirically evaluated at 0.33. Expressing this equation at all wavelengths, and assuming that Beer's law holds for absorption, leads to a matrix equation for spectral reflectance as a function of concentrations of spectral endmembers [Pilorz and Davis, 1990]:

$$R_M(Ac + b) = kb \quad (2a)$$

or

$$c = (A^T A)^{-1} A^T (R_M^{-1} - I) kb \quad (2b)$$

R_M in equations 2a and b is a square matrix with reflectances at observed wavelengths as the diagonal entries, A is a column matrix of specific absorption coefficients at those wavelengths for some number of endmembers, c is a vector of concentrations for the endmembers represented in A, and b is a column vector of backscattering coefficients at each wavelength. Clearly, accurate evaluation of c from this expression must involve simultaneous estimation of the concentration vector and spectral backscattering, although that will not be discussed in the present text.

Use of the above expression with remotely sensed data requires additional formulae for propogation of flux across the water surface and expression of the upwelled radiance in terms of the reflectance. In the following expression [Gordon and Clark, 1981; Austin, 1974], L_u represents the upwelled radiance just above the surface, ρ and ρ_b represent the fresnel transmittances of the surface from above and below, n is the index of refraction of water, and Q is roughly equal to the inverse of the average upwelling cosine, used for conversion to radiance units:

$$L_u = E_d (1-\rho)(1-\rho_b) R / Q n^2 \quad (3)$$

METHODS AND DATA

The purpose of our investigation is to examine the feasibility of applying equations (1) through (3) to spectral decomposition through in-situ determination of the magnitudes and variances of individual terms as well as empirical testing of the reflectance model itself.

On 19 October 1989 in-water optical measurements were made on the R/V Shana Rae as part of an experiment in Monterey Bay in conjunction with an AVIRIS overflight taken the previous day. The research area is shown in Figure 2, where the overlaid boxes correspond to the scenes used in this analysis. Optical data were collected with a Bio-Optical Profiling System (BOPS), an updated version of the BOPS developed by Smith et al. [Smith et al., 1984]. The heart of the BOPS is a Biospherical Instruments MER-1048 Spectroradiometer which measures upwelling and downwelling spectral irradiance and upwelling spectral radiance. The MER-1048 also has sensors for Photosynthetically Available Radiation (PAR), depth, tilt, and roll. In addition, chlorophyll fluorescence was measured with a Sea-Tech fluorometer and beam transmission with a Sea-Tech 25-cm transmissometer. The BOPS data were filtered to remove obvious data spikes and then binned into one-meter averages over depth.

These data were used for calculation of optical parameters as well as chlorophyll concentrations for use in checking equations (1) through (3). Figure 3 shows plots of R,

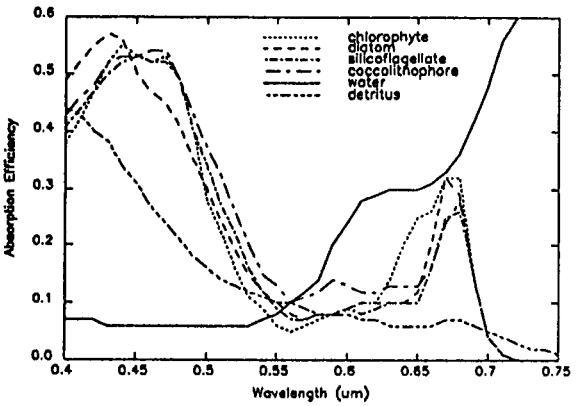

Fig. 1. Absorption efficiencies plotted versus wavelength for some classes of in-water constituents.

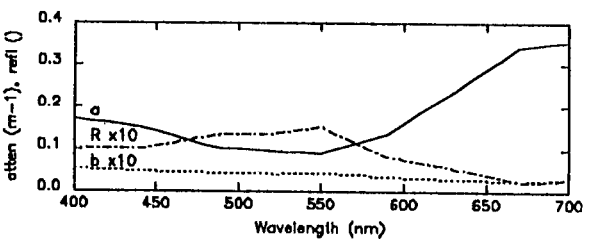

Fig. 3. Spectral absorption (a), reflectance (R), and backscattering (b) plotted versus wavelength. Reflectance is relatively smaller than absorption and inversely proportional to it.

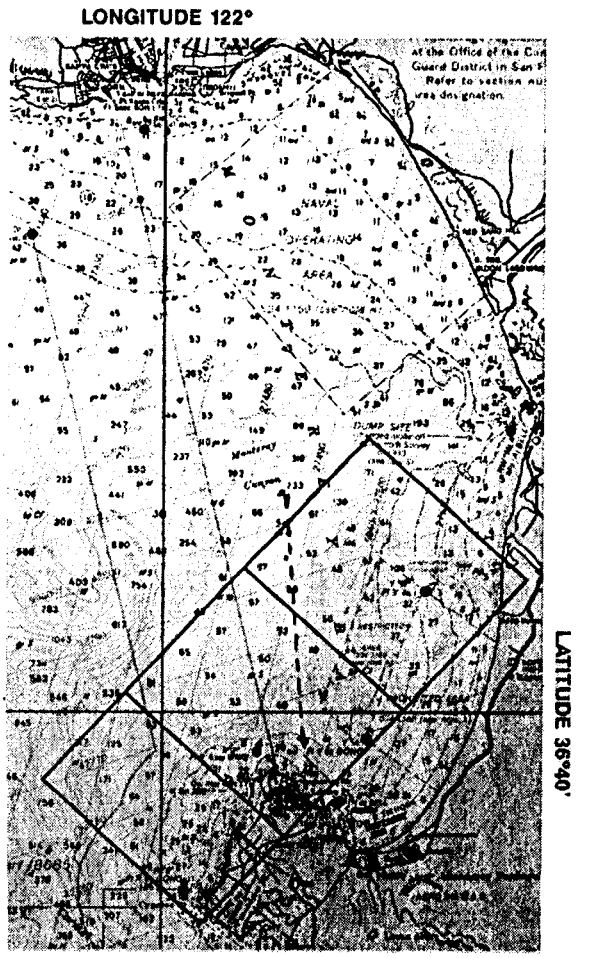

Fig. 2. Monterey Bay, California. Boxes correspond to AVIRIS scenes taken on 18 October, 1989. Dotted line shows transect plotted in figure 5.

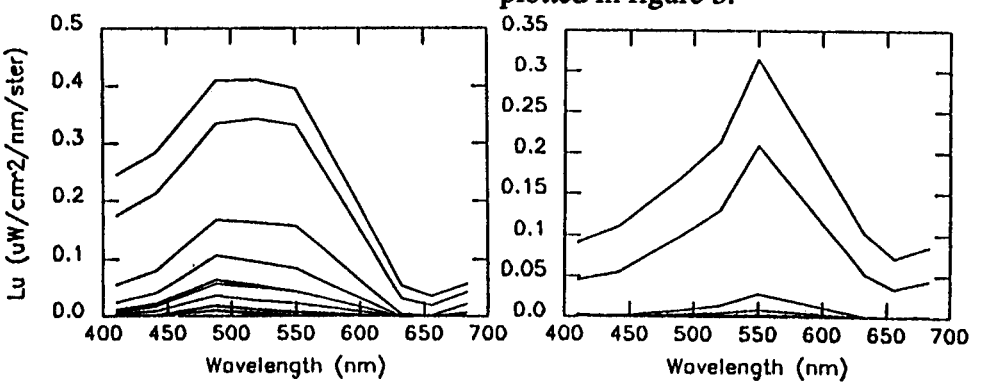

Fig. 4. (a) Upwelling radiance plotted versus wavelength from the station at 36°39.1'N, 121°55.8'W. Separate lines correspond to 5 m increments in depth. (b) Same as in (a) except for the station at 36°47.8'N, 121°50.8'W.

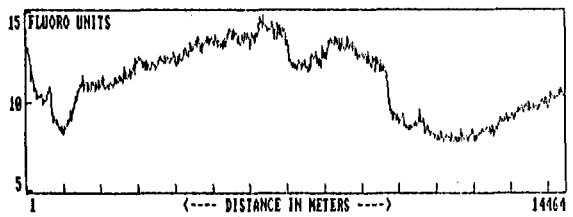

Fig. 5. Surface fluorometer measurements taken from the transect marked in figure (2).

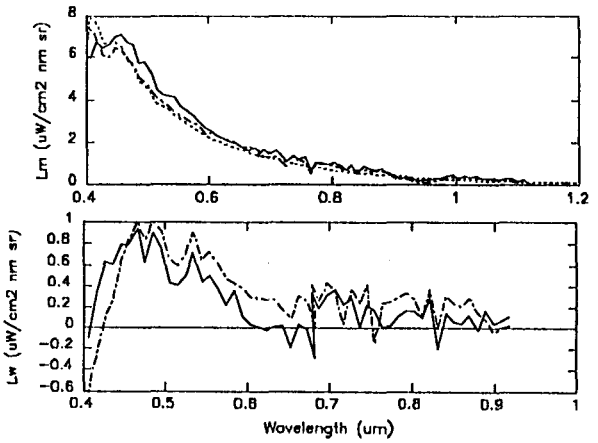

Fig. 6. (a) Spectrum from the scene plotted versus wavelength (solid), and path radiances calculated from LOWTRAN 7 and a single scattering model (dotted). (b) Difference between the received radiance and the calculated path radiances.

b, and a as functions of wavelength, evaluated at a station off Monterey, California, at 36° 39.1' N and 121° 55.8'W. This shows the general inverse dependence of R upon a, as well as the small magnitude and spectrally flat properties of the backscattering spectrum, b.

Figures 4a and 4b show upwelling radiances below the surface from low and high chlorophyll stations, in which the effect of increased chlorophyll can be clearly seen as a depression of the reflectance in the 400 to 450 nm region in Figure 4b. The surface pigment levels correspond to approximately 2.5 and 6.5 mg chlorophyll + phaeopigment/m^3 for figures (a) and (b) respectively, and even though the absorption was due to different phytoplankton groups at each station, the magnitude of the signal is characteristic of that which we would need to discriminate. A difference of 0.17 $\mu W/cm^2$ nm sr at 450 nm for a chlorophyll variation of 3 or 4 mg/m^3 implies that we would need to distinguish signals on the order of 0.05 $\mu W/cm^2$ nm sr in order to determine chlorophyll fluctuations on the order of 1 mg/m^3.

Figure 5 is included to give an idea of the spatial structure of the chlorophyll field, taken along a 14 km transect running diagonally across the image (Figure 2). The fluorometry is a linear function of chlorophyll, where the peaks of 15 fluoro units correspond to approximately 2.7 mg chlorophyll/m^3 (3.5 mg chlorophyll + pigment/m^3) and the low of 7.5 fluoro units corresponds to approximately 1.3 mg chlorophyll/m^3 (1.9 mg chlorophyll + phaeopigments/m^3).

The AVIRIS data from the scene were taken at a solar zenith angle of approximately 48°, hence, they have an unfavorably small S/N. Figure 6 shows a sample spectrum from near the middle of the scene with path radiances calculated using LOWTRAN 7 and a single scattering model. The residual signal (Figure 6b) ranges from 2 to 15% of that received at the sensor, hence has a S/N ranging of 0.1 to 0.02 times that of the received signal.

Suppose that the S/N was 90:1 at 500 nm, then the standard deviation on a signal of 6 $\mu W/cm^2$ nm sr would be about 0.075 $\mu W/cm^2$ nm sr, or roughly one DN. In actuality, from factors due mostly to aircraft-induced periodicities, we observe a standard deviation of roughly 0.26 $\mu W/cm^2$ nm sr, or about 3.5 DN (S/N of about 25:1), as compared to an atmospherically corrected signal on the order of 0.8 $\mu W/cm^2$ nm sr. This gives an effective S/N of slightly better than 3:1 for the signal, implying that discernment of a 0.05 $\mu W/cm^2$ nm sr signal would require binning to a spatial resolution of 100 m, or 5 x 5 pixels, in the absence of correlation effects within the noise.

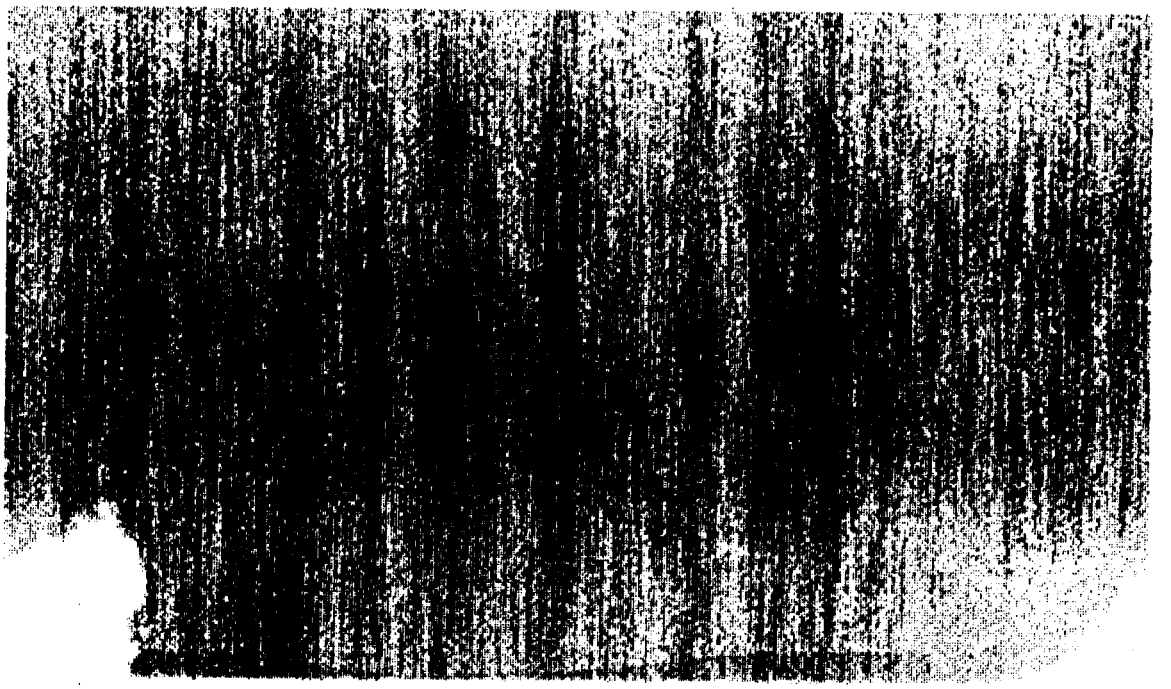

Fig. 7. Data from the calibrated AVIRIS scene corresponding to the Eastern two boxes in Figure 1. Band 12 is shown stretched linearly two standard deviations about the mean. Linear grey scale is used for this and other images.

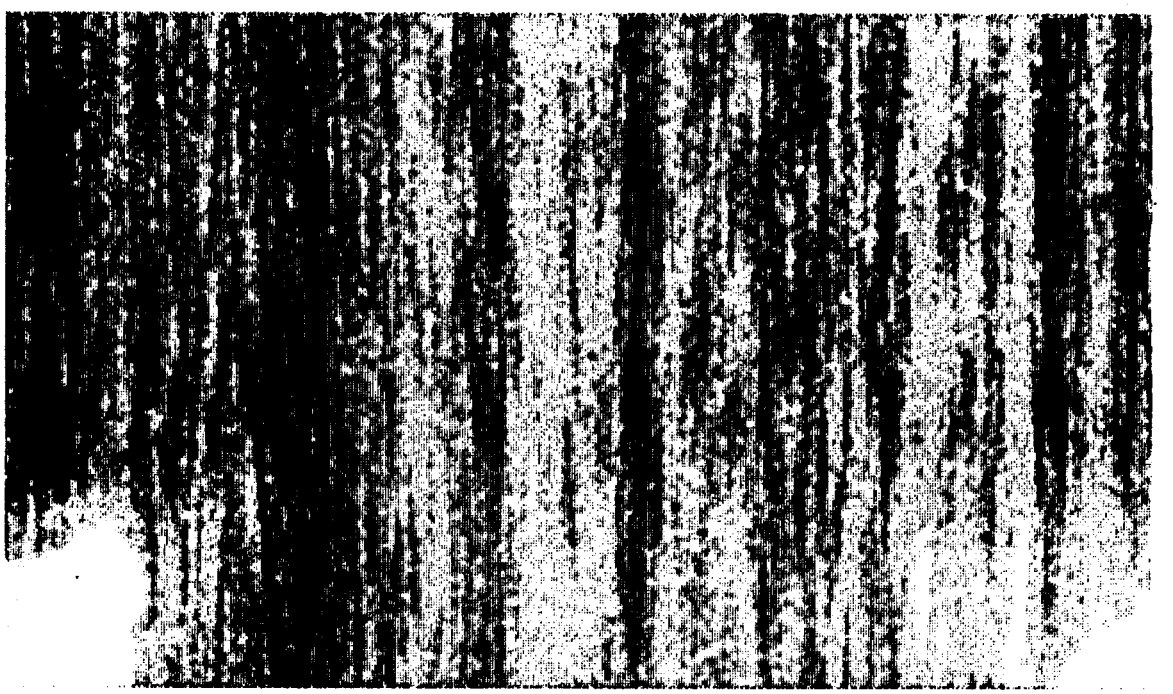

Fig. 8. Ratio of bands 15 to 12 from the AVIRIS scene, stretched linearly 2 standard deviations about the mean. This should give some idea of chlorophyll concentrations, as band 12 is more sensitive to chlorophyll than band 15.

Examination of the calibrated data, Figure 7, shows a vignetting effect of approximately 0.15 $\mu W/cm^2$ sr nm in the cross-track direction. This resulted from the use of a single vignetting profile to correct all of the bands in spectrometer A, whereas in this region the vignetting is spectrally dependent. New vignetting profiles at each band have since been generated from integrating sphere data, and in the future these will be used routinely during data processing.

Application of a chlorophyll ratio algorithm using bands 15 and 12 (Figure 8) decreases the vignetting effect. Large features are apparent in this image; however, they are obfuscated by wide vertical striping not present in the raw data. This is due to subtraction of a dark current from each line during processing which was not representative of the actual dark current during the data acquisition for that line. This small effect is significant for dark scenes. Its appearance in this data has lead to changing the size of the boxcar filter applied to the dark current prior to its removal during data calibration, as well as to the investigation of modifications to the instrument which would allow collection of more dark current data during the scan flyback.

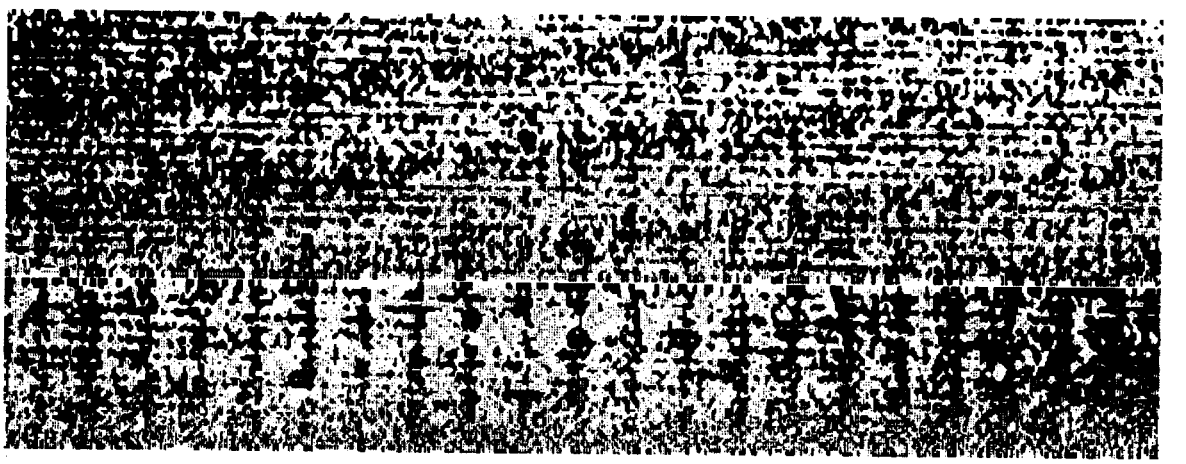

Fig. 9. One line of data from the AVIRIS scene. Bands 1 to 80 are along the vertical scale, with 614 cross-track samples along the horizontal. Data are smoothed by 3 pixels cross track and by 2 bands spectrally. Each band (row) has had the mean subtracted and is divided by its standard deviation.

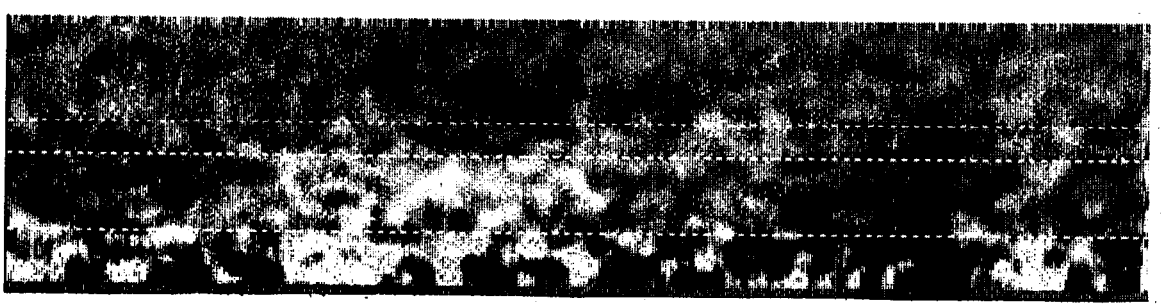

Fig. 10. Along track nadir transect from the AVIRIS scenes with bands 1 to 80 along the vertical axis and 1024 lines along the horizontal axis. Each row has had its mean subtracted and been divided by its standard deviation. Dotted lines correspond to bands 5, 12, and 15. Large features between bands 5 and 12 correspond to chlorophyll low and high, respectively, moving from left to right.

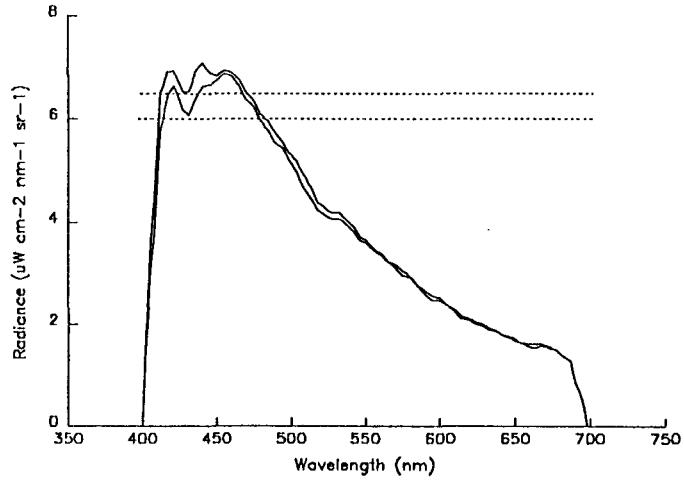

Fig. 11. Sample spectra from low and high chlorophyll areas within the scene, binned by 100 pixels (10 x 10) spatially. Dotted lines are at 6.0 and 6.5 $\mu W/cm^2$ nm sr, and are intended to show the magnitude of the chlorophyll signature.

Viewing of a dark target has proven useful in finding periodicities in the signal as well. Figure 9 shows one line of data with spectral bands 1 to 80, in which multiple periodicities are apparent as vertical and diagonal striping. The signals causing these are both time sequential (diagonal bands) as well as scan related (vertical bands) and have individual amplitudes of up to more than 2 DN. Comparison with integrating sphere data has shown that most of this coherent noise is due to aircraft operation. The problems are twofold for viewing dark targets, in that the periodicities increase the standard deviation of the data (reducing the S/N), as well as preclude the use of binning to beat down the S/N. Also, due to the large number of frequencies and the mixing of some of these features with the vignetting profile, notch filtering was not possible with this data set.

Examination of a smoothed along track transect (Figure 10) shows the spectral variation from West to East across the scene. Patches of high chlorophyll would be seen at this resolution as relative lows in bands 1 to 12, with higher bands remaining relatively stable. Such a large high and low are evident moving across the scene from West to East (left to right). The issue of dark current effect, however, as well as a slight diagonal skew to the high pixels, suggests the possibility that this is at least partially an artifact due to periodic noise. Thus, caution is required in interpretation of this feature as being chlorophyll induced. Smoothed spectra taken from these areas, also along this transect, are shown in Figure 11, demonstrating that a signal may be extracted from the data.

CONCLUSIONS

AVIRIS and HIRIS data will undoubtedly be extremely useful for the study of the ocean's role in the world carbon cycle, as well as in understanding coastal waters whose complex reflectances elude the capability of low resolution instruments. In-situ studies as well as modelling indicate that the use of this data in the manner desired will require a Noise Equivalent Delta Radiance (NEDR) on the order of 0.05 $\mu W/cm^2$ nm sr; well below the present stated requirements for AVIRIS. This study has shown that, nonetheless, AVIRIS is presently on the borderline for meeting the S/N requirements for ocean viewing.

Typical ocean albedos of 1 to 2% lead to a path radiance contribution of usually 90% to the radiance received at the sensor. Calibration sensitivities for this study ranged from 0.4 to 0.05 $\mu W/cm^2$ nm sr in the blue spectrum, with a NEDR ranging from 0.8 to 0.1. The net result is that without substantial data binning, the desired signal is sufficiently less than the noise in the signal, and care must be taken to limit coherent noise as much as possible.

Substantial contributions to the NEDR from aircraft operation were apparent in this data, as well as patterns due to spectrally dependent vignetting and dark current filtering. These problems are especially bothersome in that they will not be removed by binning, and

are not always obvious in themselves. The steps which have been taken to remedy these problems are increased shielding on instrument cables, routine application of spectrally dependent vignetting profiles, and modification of the filter size applied to the dark current during processing. In addition, the AVIRIS engineering team has suggested several relatively inexpensive modifications to the instrument which, if implemented, could produce a factor of 2 to 4 increase in S/N in the blue spectral region by the 1991 or 1992 season. These include modifying the blaze on the diffraction grating for spectrometer A, changing some spectrally dependent optical coatings in the foreoptics, and replacing the line array for spectrometer A with one of higher efficiency. The results of this study suggest that such improvements would be extremely beneficial for future oceanographic studies.

ACKNOWLEDGMENTS

The authors would like to thank the AVIRIS engineering team in general and Rob Green in particular for their many invaluable suggestions and keen interest in increasing the performance capabilities of the instrument. The research described in this paper was carried out at the Jet Propulsion Laboratory, California Institute of Technology, and was funded by NASA grant FY-413-18-00-06-45 to C.O. Davis and the HIRIS project.

REFERENCES

Austin, R. "The Remote Sensing of Spectral Radiance from below the Ocean Surface," Optical Aspects of Oceanography, N.G. Jerlov and E.S. Nielsen [eds.], pp. 314-344, Academic, 1974.

Gordon, H. and D. Clark, "Clear Water Radiances for Atmospheric Correction of Coastal Zone Color Scanner Imagery," Applied Optics, Vol. 20, No. 24, pp. 4175-4180, 1981.

Gordon, H. et al., "Computed Relationships between the Inherent and Apparent Properties of a Flat Homogeneous Ocean," Applied Optics, Vol. 14, No. 2, pp. 417-427, 1975.

Kirk, J., "Monte Carlo Study of the Nature of the Underwater Light Field in, and the Relationships between Optical Properties of Turbid Yellow Waters," Aust. J. Mar. Freshwater Res., Vol. 32, pp. 517-532, 1981.

Kirk, J., Light and Photosynthesis in Aquatic Ecosystems, Cambridge Press, NY, 1983.

Morel, A. and L. Prieur, "Analysis of Variations in Ocean Color," Limnol. Oceanogr., Vol. 22, No. 4, pp. 709-722, 1977.

Pilorz, S. and C. Davis, "Spectral Decomposition of Sea Surface Reflected Radiance," Proc. IGARSS 1990, Vol. 1, pp. 345-348, IEEE,1990.

Preisendorfer, R., Hydrologic Optics, U.S. Dept of Commerce NOAA publ. (6 volumes), 1976.

Scientific Committee on Oceanic Research, "The Joint Global Ocean Flux Study, Report of the First Session of the SCOR Committee for JGOFS," Miami, FL, January 25-28, 1988.